Crystal Structure and Magnetic Properties of the Trilayered Perovskite $Sr_4Rh_3O_{10}$: A New Member of the Strontium Rhodate Family

Kazunari Yamaura,*,† Qingzhen Huang,‡ David P. Young,§ and Eiji Takayama-Muromachi†

Superconducting Materials Center, National Institute for Materials Science, 1-1 Namiki, Tsukuba, Ibaraki 305-0044, Japan, NIST Center for Neutron Research, National Institute of Standards and Technology, Gaithersburg, Maryland 20899, and Department of Physics and Astronomy, Louisiana State University, Baton Rouge, Louisiana 70803

Received June 4, 2004

The trilayered perovskite $Sr_4Rh_3O_{10}$ is reported for the first time. High-pressure and high-temperature heating (6 GPa and 1500 °C) brought about successful preparation of a polycrystalline sample of the expected member at $n = 3$ of $Sr_{n+1}Rh_nO_{3n+1}$. Neutron-diffraction studies revealed the orthorhombic crystal structure (*Pbam*) at room temperature and 3.4 K. Local structure distortions rotationally tilt the RhO_6 octahedra ∼12° in the perovskite-based blocks along the *c*-axis, and approximately a 20% disorder was found in the sequence of the alternating rotational tilt. The sample was also investigated by measurements of specific heat, thermopower, magnetic susceptibility, and electrical resistivity. The data clearly revealed enhanced paramagnetism and electrically conducting character, which reflected the nature of the correlated $4d^5$-electrons of Rh^{4+}. However, no clear signs of magnetic and electrical transitions were observed above 2 K and below 70 kOe, providing a remarkable contrast to the rich electronic phenomena for the significantly relevant ruthenate $Sr_4Ru_3O_{10}$.

Introduction

Perovskite families in the transition-metal oxides are scientifically attractive and may play an important role in future engineering applications. This is due to a wide variety of significant magnetic and electronic properties strikingly illustrated by high-T_c superconductivity in cuprates,[1] quantum magnetic character in ruthenates,[2] and strongly correlated features in manganates.[3] For the purpose of understanding the common physics of the materials, numerous intensive studies focused on the materials in both experimental and theoretical ways. So far, consequences addressed in many of the studies highlight the merit of the discovery of novel materials, which show unusual characters or remarkable levels of performance. We therefore searched for new members of the perovskite family to aid our understanding of the physics. In the past few years we have spent much effort in synthesizing perovskite-based 4d element oxides by means of solid-state reaction at elevated pressure in the several GPa range. As such, the high-pressure and high-temperature heating offer advantages over conventional synthesis techniques.[4−6]

In the ternary Sr−Rh−O system, several compounds were already reported, $Sr_{0.75}Rh_4O_8$,[7] $SrRh_2O_4$,[8] $Sr_6Rh_5O_{15}$,[9,10] Sr_2RhO_4,[11,12] and Sr_4RhO_6,[13] which were synthesized by rather conventional methods and seem well-characterized. Recently, two new members were added to the rhodate system, which were prepared by a high-pressure method: the perovskite $SrRhO_3$[14] and the bilayered $Sr_3Rh_2O_7$.[15] At the end of the high-pressure studies, it was clear that the three compounds form a novel perovskite family as expressed by the general formula $Sr_{n+1}Rh_nO_{3n+1}$ (n = 1, 2, and ∞), indicating this must be a Ruddlesden−Popper series.[16,17] It was also stressed that all the members were magnetically and electrically active, because the oxygen-

* To whom correspondence should be addressed. Fax. +81−29−860−4674. E-mail: YAMAURA.Kazunari@nims.go.jp.
† National Institute for Materials Science.
‡ National Institute of Standards and Technology.
§ Louisiana State University.

(1) Anderson, P. W. *The Theory of Superconductivity in the High-Tc Cuprate Superconductors*; Princeton Series in Physics; Princeton University Press: Princeton, NJ, 1997.
(2) Mackenzie, A. P.; Maeno, Y. *Rev. Mod. Phys.* **2003**, *75*, 657.
(3) Tokura, Y.; Nagaosa, N. *Science* **2000**, *288*, 462.
(4) Poeppelmeier, K.; Navrotsky, A.; Wentzcovitch, R. *Perovskite Materials*; Material Research Society: Warrendale, PA, 2002.
(5) McMillan, P. F. *Nature Mater.* **2002**, *1*, 19.
(6) Demazeau, G. *J. Phys. Cond. Matt.* **2002**, *14*, 11031.
(7) Plaisier, J. R.; van Vliet, A. A. C.; IJdo, D. J. W. *J. Alloys Compd.* **2001**, *314*, 56.
(8) Horyn, R.; Bukowski, Z.; Wolcyrz, M.; Zaleski, A. J. *J. Alloys Compd.* **1997**, *262*, 267.
(9) Stitzer, K. E.; El Abed, A.; Darriet, J.; zur Loye, H.-C. *J. Am. Chem. Soc.* **2001**, *123*, 8790.
(10) Claridge, J. B.; zur Loye, H.-C. *Chem. Mater.* **1998**, *10*, 2320.
(11) Itoh, M.; Shimura, T.; Inaguma, Y.; Morii, Y. *J. Solid State Chem.* **1995**, *118*, 206.
(12) Shimura, T.; Itoh, M.; Nakamura, T. *J. Solid State Chem.* **1992**, *98*, 198.
(13) Vente, J. F.; Lear, J. K.; Battle, P. D. *J. Mater. Chem.* **1995**, *5*, 1785.
(14) Yamaura, K.; Takayama-Muromachi, E. *Phys. Rev. B* **2001**, *64*, 224424.
(15) Yamaura, K.; Huang, Q.; Young, D. P.; Noguchi, Y.; Takayama-Muromachi, E. *Phys. Rev. B* **2002**, *66*, 134431.
(16) Ruddlesden, S. N.; Popper, P. *Acta Crystallogr.* **1958**, *11*, 54.
(17) Ruddlesden, S. N.; Popper, P. *Acta Crystallogr.* **1957**, *10*, 538.

10.1021/cm0491072 CCC: $27.50
Published on Web 08/04/2004

coordinated rhodium ions were formally tetravalent and then each had an unpaired electron ($t_{2g}^5e_g^0$ configuration).[18] As the all compounds in $Sr_{n+1}Rh_nO_{3n+1}$ formally form a spin-$^1/_2$ system, the appearance of evident quantum critical characters could be highly expected in the vicinity of $Sr_{n+1}Rh_nO_{3n+1}$ or under physically extreme conditions.[19,20] In fact, past studies on the $n = \infty$ compound suggested a substantial influence from quantum critical fluctuations.[14,20]

Being motivated to explore the perovskite rhodate family, we have been attempting to synthesize an expected compound at $n = 3$ in the general expression above. Although the possible formation of $Sr_4Rh_3O_{10}$ was implied in our preliminary studies, a pure bulk sample had never been prepared thus far. Samples of $Sr_4Rh_3O_{10}$ in the early preparations always contained $SrRhO_3$ or other impurity phases. Even polycrystalline samples of the relevant ruthenate $Sr_4Ru_3O_{10}$ never became pure, and high-pressure heating might be necessary, according to reports.[21−25] These facts were indicative of problems with syntheses of the high-*n*-numbered Ruddlesden−Popper compounds, except the infinity-numbered one. We were then engaged in optimizing the heating conditions, improving the quality of the starting materials, and testing a variety of nominal compositions. As a result, a perfect single-phase sample was never achieved; however, the amount of impurities were reduced to an acceptable level for several studies, including magnetic susceptibility measurements and neutron diffraction analysis.

In this paper, the structure and the magnetic properties of a new member of the rhodate perovskite family, $Sr_4Rh_3O_{10}$, are reported, and a systematic trend of the magnetism of the family is compared with that of the significantly relevant ruthenate family, which has previously received the most recent attention.

Experimental Section

Sample Preparation. Polycrystalline samples were prepared in a platinum cell (6.8 mm in diameter, 0.2 mm in thickness, and approximately 5 mm in height) by solid-state reaction at high pressure. Fine and pure powders of SrO_2, Rh_2O_3, and Rh were employed as starting materials; SrO_2 was prepared as follows.[26] $SrCl_2{\cdot}6H_2O$ was dissolved in a sufficient amount of water, followed by dropwise addition of ammonia solution and H_2O_2 solution. The precipitation was washed with water after being filtered and then dried in oxygen at 150 °C for approximately 3 h, resulting in a white powder. X-ray diffraction analysis characterized the powder to be SrO_2. The oxygen content was studied by reduction to strontium monoxide in thermogravimetric analysis (TGA) by heating in 3% hydrogen/argon at a heating rate of 5 °C/min to 800 °C and holding for 8 h. The weight loss data suggested the stoichiometric oxygen content (2.04 oxygens per mol). The Rh_2O_3 powder was obtained by heating the Rh powder (99.9%) in oxygen at 1000 °C overnight. TGA and X-ray diffraction analysis characterized the powder to be Rh_2O_3.[27] The estimated oxygen content was 3.01 mol per the formula. Alternatively, commercial powder Rh_2O_3 (99.9%) was also used. The Rh powder was annealed in argon at 1000 °C for 3 h before use. The powders were mixed at the stoichiometric or several nonstoichiometric ratios and placed into the platinum cell. The cell was heated at a fixed temperature in the range between 1300 and 1600 °C for 1 h at 6 GPa and then quenched to room temperature by turning off the heater current before releasing the pressure. A detailed technical description of our high-pressure apparatus is available elsewhere.[28,29] The polycrystalline samples were black in color and retained a pellet shape. Each face of the sintered pellet was polished carefully in order to remove any possible contaminations from chemical reactions with the platinum cell. A typical sample mass obtained was ~0.4 g.

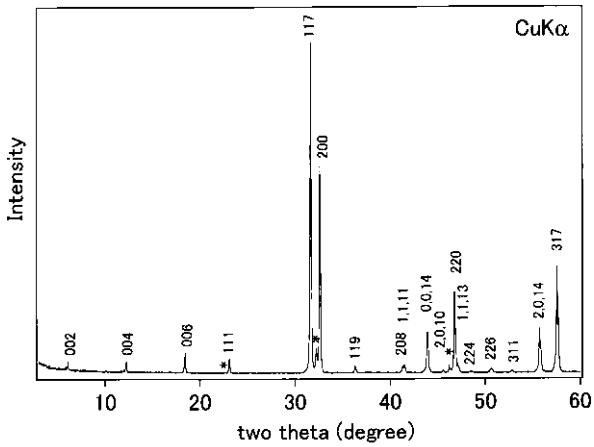

Figure 1. Powder X-ray diffraction profile of the $Sr_4Rh_3O_{10}$ sample, measured at room temperature. The peaks are indexed on the basis of a primitive tetragonal cell [$a = 5.493(1)$ Å and $c = 28.83(1)$ Å] for clarity. Star marks indicate peaks for $SrRhO_3$.

The samples were examined for quality with powder X-ray (Cu Kα) diffraction in a high-resolution powder diffractometer (RINT-2000 system, RIGAKU, Co), which was equipped with a graphite monochromator on the counter side. In Figure 1, the X-ray diffraction pattern at room temperature for the best quality sample of $Sr_4Rh_3O_{10}$ is shown. All major peaks were assigned to a tetragonal unit cell with reasonable lattice parameters [$a = 5.493(1)$ Å and $c = 28.83(1)$ Å] for the expected member. However, a trace of $SrRhO_3$ was detected in the X-ray survey and also in an electron probe microanalysis (EPMA, mentioned later). The identified impurity indeed gave a reasonable account for the small peaks left in the analysis, as shown by small stars in Figure 1. Because the structure, magnetic, and electronic properties of the minor impurity were well-known, its contribution to the present data could be interpreted.[14] We therefore decided to use this sample and an equally pure sample for further studies, including neutron diffraction and magnetic properties measurements.

Here we describe experimental details of the sample preparation. All the products were qualitatively studied by the X-ray diffraction method. The X-ray survey was, however, unable to establish a reasonable phase-equilibrium picture of the quasibinary system SrO−RhO_2 at high pressure. Probably,

(18) Lee, Y. S.; Lee, J. S.; Noh T. W.; Byun D. Y.; Yoo, K. S.; Yamaura, K.; Takayama-Muromachi, E. *Phys. Rev. B* **2003**, *67*, 113101.
(19) Sachdev, S. *Quantum Phase Transitions*; Cambridge University Press: New York, 1999.
(20) Singh, D. J. *Phys. Rev. B* **2003**, *67*, 054507.
(21) Xin, Y.; Cao, G.; Crow, J. E. *J. Cryst. Grow.* **2003**, *252*, 372.
(22) Cao G.; Balicas L.; Song W. H.; Sun Y. P.; Xin Y.; Bondarenko V. A.; Brill J. W.; Parkin S.; Lin X. N. *Phys. Rev. B* **2003**, *68*, 174409.
(23) Crawford, M. K.; Harlow, R. L.; Marshall, W.; Li, Z.; Cao, G.; Lindstrom, R. L.; Huang, Q.; Lynn, J. W. *Phys. Rev. B* **2002**, *65*, 214412.
(24) Cao, G.; McCall, S. K.; Crow, J. E.; Guertin, R. P. *Phys. Rev. B* **1997**, *56*, R5740.
(25) Cava R. J.; Zandbergen H. W.; Krajewski J. J.; Peck W. F.; Batlogg B.; Carter S.; Fleming R. M.; Zhou O.; Rupp L. W. *J. Solid State Chem.* **1995**, *116*, 141.
(26) Bernal, J. D.; Diatlowa E.; Kasarnowsky J.; Reichstein S.; Ward A. G. Z. *Kristallogr. A* **1935**, *92*, 344.
(27) Leiva, H.; Kershaw, R.; Dwight, K.; Wold, A. *Mater. Res. Bull.* **1982**, *17*, 1539.
(28) Kanke, Y.; Akaishi, M.; Yamaoka, S.; Taniguchi, T. *Rev. Sci. Instrum.* **2002**, *73*, 3268.
(29) Yamaoka, S.; Akaishi, M.; Kanda, H.; Osawa, T.; Taniguchi, T.; Sei, H.; Fukunaga O. *J. High-Pressure Inst. Jpn.* **1992**, *30*, 249.

sample quality depended on multiple factors not only pressure and temperature but also others, such as the purities of the starting materials and homogeneity of pressure and temperature in the platinum cell. Besides, efficiency of quenching may also affect the sample quality. In a series of sample preparations, a starting composition slightly off-stoichiometry, Sr:Rh:O = 4:3.4:11.016 (2% oxygen excess), resulted in the best quality thus far achieved, while the stoichiometric composition also resulted in an equivalent quality after the Rh_2O_3 powder was switched to the commercial powder. The former Rh_2O_3 powder might be unsatisfactory; however, one possibility was implied about chemical reactivity, which might be increased due to the reduced particle size of the commercial powder. The TGA and the X-ray study did not clearly show what was significant for the experimental inconsistency.

Despite further efforts, improvement of the sample quality reached a saturation level. We therefore decided to use the two best-quality samples for further studies, even though those samples included a few percent of $SrRhO_3$ and possibly other undetected impurities. The former sample (Figure 1) was used for magnetic and electrical measurements, and the latter was used for the neutron diffraction study. The major heating conditions for the both samples were identical: the elevated temperature and pressure were 1500 °C and 6 GPa, respectively. As the synthesis situation is rather complicated, further studies would be necessary to further improve the sample quality of $Sr_4Rh_3O_{10}$.

The polycrystalline sample of Sr_2RhO_4 was prepared as well. The sample was heated at 1450 °C for 1 h at 6GPa. The starting composition was at the stoichiometric ratio using the commercial Rh_2O_3 powder. The X-ray diffraction study of the sample confirmed the formation of Sr_2RhO_4.[11] The measured lattice parameters of the tetragonal unit cell at room temperature were $a = 5.453(1)$ Å and $c = 25.78(1)$ Å, which matched well with the data in the literature.[11]

Chemical Analysis. A piece of the selected $Sr_4Rh_3O_{10}$ sample used for the physical property measurements was studied by energy-dispersive X-ray spectroscopy (EDS; AKASHI, ISI-DS-130) at the accelerated voltage of 10 kV in a scanning electron microscope. Every X-ray spectrum at more than 10 points of the polished surface clearly revealed the absence of platinum contamination. No platinum signal was detected above background level, indicating that the platinum concentration was less than 0.1 wt %. We recognized only Sr, Rh, O, and C (coating material) contributions in the spectra.

The EPMA (JEOL, JXA-8600MX) was also carried out on the same $Sr_4Rh_3O_{10}$ sample to estimate the chemical composition of the constituent particles. Analysis was conducted for a number of particles (approximately 10 μm in the largest dimension); the average ratio of Sr to Rh was 4 to 3.01(2), although the nominal composition was off-stoichiometry. Additionally, a 1 to 1.00(2) ratio was obtained from a $SrRhO_3$ sample previously prepared,[14] indicating the accuracy of the analysis. The quantitative analysis above did not indicate a substantial nonstoichiometry of the metal in the compound.

Physical Properties Measurements. The magnetic susceptibility was measured in a commercial apparatus (Quantum Design, PPMS-XL) at 50 kOe between 2 and 390 K. The data for $SrRhO_3$ were taken from our previous report,[14] and an older $Sr_3Rh_2O_7$ sample was restudied at the same conditions. Although the $Sr_3Rh_2O_7$ sample was left in a dry jar for approximately 20 months, an X-ray survey did not detect any signs of decomposition. Indeed, the newly obtained data were consistent with those previously measured at 70 kOe.[15]

A piece of each sample pellet of $Sr_4Rh_3O_{10}$ and Sr_2RhO_4 was cut out into a bar shape. The electrical resistivity of the bars was then measured between 2 and 390 K by a conventional four-point method in a commercial apparatus (Quantum Design, PPMS system). The ac-gauge current at 30 Hz was 1 mA for the $Sr_4Rh_3O_{10}$ sample and 50 mA for the Sr_2RhO_4 sample. Silver epoxy was used to fix fine platinum wires (~30 μm diameter) at four locations along the bar-shaped sample. Specific-heat measurements were conducted on another piece of each pellet in the PPMS system with a time-relaxation method over the temperature range between 1.8 and 10.3 K. The thermopower of the samples was measured in the PPMS system between 5 and 300 K with a comparative technique using a constantan standard.

Neutron Diffraction. The selected $Sr_4Rh_3O_{10}$ sample for neutron diffraction study was ground in an agate mortar. The sample powder (~0.4 g) was set in the BT-1 high-resolution diffractometer at the NIST Center for Neutron Research, employing a Cu(311) monochromator. The survey was conducted at room temperature and 3.5 K. Because the sample mass was fairly small, it took a long period, approximately 2.5 days per each run, until intensities were above an acceptable level. Collimators with horizontal divergences of 15′, 20′, and 7′ of arc were used before and after the monochromator, and after the sample, respectively. The calibrated neutron wavelength was $\lambda = 0.15396(1)$ nm, and drift was negligible during the data collection. The intensity of the reflections was measured at 0.05° steps in the 2θ range between 3 and 168°. Neutron scattering amplitudes used in data refinements were 0.702, 0.593, and 0.581 ($\times 10^{-12}$ cm) for Sr, Rh, and O, respectively.

Results and Discussion

The neutron diffraction study revealed details of the average structure of $Sr_4Rh_3O_{10}$. Rietveld refinements were attempted on the powder profiles with the GSAS program.[30] Because the significantly relevant systems $Sr_3Rh_2O_7$ and $SrRhO_3$ share a common structure model with each corresponding ruthenate, the structurally intermediate $Sr_4Rh_3O_{10}$ was expected to share the trilayered structure model with the ruthenate $Sr_4Ru_3O_{10}$ as well. We then utilized the ruthenate model [*Pbam* at $a = 5.5280(11)$ Å, $b = 5.5260(11)$ Å, and $c = 28.651(6)$ Å] for initial structure parameters in the refinement analysis.[23] Within the *Pbam* model, the solution reached a fairy reliable level after embedding the disorder factors into the model (see below). The result clearly supported the *Pbam* model for the structure of $Sr_4Rh_3O_{10}$ as well as $Sr_4Ru_3O_{10}$. However, we do not rule out the possibility of closely related models such as *Bbcm*, as discussed in the former study.[23] In the analysis, we considered that the structure in fact has an orthorhombic symmetry with a slight difference between the *a*-axis and *b*-axis parameters. However, we needed to constrain some parameters to be tetragonal due to the low-laying intensity profiles. To confirm the exact structure symmetry, a synchrotron experiment would be helpful. Details of the analysis and the results are summarized in Tables 1 and 2. The raw neutron profile at 3.4 K and the analyzed curves are shown in Figure 2 as an example.

One of the major issues in this structure survey was to elucidate possible stacking disorders, which are inherent in layered materials. In our previous study of the relevant system $Sr_3Rh_2O_7$, approximately 8% disorder was detected along the *c*-axis, which was characterized by an error about directions of alternating rotation tilt of RhO_6 octahedra.[15] This result implied that similar disorder might be in $Sr_4Rh_3O_{10}$. To test this possibility, O3′ and O4′ atoms were introduced with some constraints, which led to the same type of errors.[15] In refinements, the occupancy factor of the hypothetical atoms was expected to be a measure of the frequency of the errors.

(30) Larson, A. C.; Von Dreele, R. B. *Los Alamos National Laboratory Report* No. *LAUR086-748*, 1990.

Table 1. Crystallographic Data and Structure Refinement for $Sr_4Rh_3O_{10}$

empirical formula	$Sr_4Rh_3O_{10}$
formula weight	819.19
temperature	room temperature (first lines) and 3.5 K (second lines)
neutron wavelength	1.5396 Å
diffractometer	BT-1 at the NIST Center for Neutron Research
2θ range used	10°−155° in 0.05° steps
crystal system	orthorhombic
space group	*Pbam*
lattice constants[a]	a = 5.49353(47) Å 5.47470(15) Å
	b = 5.49353 Å 5.47470 Å
	c = 28.8004(26) Å 28.8137(12) Å
volume	869.16(13) Å^3 863.61(5) Å^3
Z	4
density (calcd)	6.260 g/cm^3 6.300 g/cm^3
observations	2899
R factors	5.91% (R_{wp}), 4.74% (R_p) 3.81 3.10

[a] Preliminary attempts without constraint resulted in undistinguishable solutions between a and b. We then decided to apply the $a = b$ constraint due to the low data resolution, as was done in the analogous ruthenium oxide $Sr_4Ru_3O_{10}$.[23] Further microscopic studies would be helpful to determine the structure symmetry much more accurately.

The incorporation of the atoms O3′ and O4′ into the *Pbam* model obviously resulted in improving quality of the solutions as exemplified in the inset of Figure 2. A quality measure of solutions (χ^2) forms a symmetrical shape in the plot against the occupancy factor (n) of O3-(O4), with a reduced value at 0.2 and 0.8 rather than at the ends. Both occupancy factors of O3 [=1 − n(O3′)] and O4 [=1 − n(O4′)] were constrained to be equal. This feature clearly indicated that approximately 20% of the perovskite blocks were out of a regular alternating rotation-tilt sequence along the c-axis in $Sr_4Rh_3O_{10}$. The solid circle in the inset is the final uncorrected solution. Since the error factors greatly improved the quality of the analysis, it seems reasonable that they occur in the true structure. The structure for the trilayered $Sr_4Rh_3O_{10}$ was then drawn on the basis of the low-temperature solutions and is displayed in Figure 3. When we consider the repetition of the stacking (−*BAB*−*B*′*A*′*B*′−*BAB*−), where *A* and *B* indicate the direction of RhO_6 rotation clockwise and counterclockwise (or vice versa), the sequence −*BAB*−*B*″*A*″*B*″−*BAB*− is the error detected above. The blocks *A*″ and *B*″ were constrained to have the same degree of rotation orientation with the *A* and *B* blocks, respectively, which have a different origin (shifted by $a/2 + b/2$ to one another).

In this structure survey, the amplitude of the rotation of the RhO_6 octahedra was estimated to be ∼12° [12.4° for the middle layer of the triperovskite block 0.5 × (180 − Rh1−O1−Rh1) and 10.9° for the two outer layers 0.5 × (180 − Rh3−O3−Rh3)], which was close to that for $Sr_3Rh_2O_7$ (10.5°).[15] The acute angle was defined to be the deviation from an ideal 180° bond caused by tilting of the RhO_6 octahedron along c-axis. The room-temperature solution indicated that the rotation was nearly temperature independent (∼11°). The amplitude for Sr_2RhO_4 was 10.3° at room temperature,[31] indicating that all the layered members (n = 1, 2, and 3) in the single family have nearly the same amplitude of the RhO_6 tilt, while the ruthenate family varies in amplitude from 0° (n = 1)[32,33] to 6.8° (n = 2)[34] to 5.6° (n = 3).[23]

The electrical resistivity data of $Sr_4Rh_3O_{10}$ are shown in Figure 4, with the data for the other members in the perovskite strontium rhodate family. The n = 3 plot is qualitatively consistent with what is expected for a metallic material, although the data are somewhat complicated by the polycrystalline nature of the sample and, to a lesser extent, the impurity. Since the metallic nature was also indicated from the thermopower measurements (Figure 5), the feature should reflect characteristics of the major portion of the sample, i.e., $Sr_4Rh_3O_{10}$. As shown in Figure 5, the Seebeck character remains nearly unaltered, quantitatively and qualitatively within the members, and consistent with a low-carrier density metallic system. The positive Seebeck coefficient indicates that the majority carrier is holelike. Although it is known that the thermopower is more sensitive than resistivity to changes in the electronic structure of materials, why the resistivity is sensitive rather than the thermopower in this materials system is unclear.

A systematic trend in the resistivity data was observed, as the curves show a rather rigid shift, nearly parallel with the vertical axis. The resistivity decreases with increasing n. The principal factor that governors this trend might be the electronic anisotropy reflected as the structural dimension increases from 2 (n = 1) to 3 (n = ∞). The lower dimensional member (n = 1) remains barely metallic, and the resistivity is higher by approximately 2 orders of magnitude than that for the n = ∞ member. Further studies, preferably on single crystals, would be necessary to firmly establish the relationship between resistivity and the structural anisotropy.

Here we should make a short statment about the discrepancy between the present data and the previously reported data by others for Sr_2RhO_4.[12,35] Each data set was obtained from independent polycrystalline samples. The present compound resistivity is approximately one magnitude lower than the other. There is no direct evidence, but we speculate that the high-pressure heating might ameliorate electrical resistive factors such as grain boundaries. In fact, a problem about "crystallinity" was mentioned in the previous report.[12] To increase the experimental accuracy of the electrical conductivity measurements further, careful studies of well quality-controlled single crystals would be significant.

In the n = 1 (Sr_2RhO_4) resistivity curve in Figure 5, a small anomaly was observed at ∼60 K, while a corresponding anomaly was seen neither in the Seebeck data nor the magnetic susceptibility data (shown later). The anomaly was reproducible. Even in the transport

(31) Vogt, T.; Buttrey, D. J. *J. Solid State Chem.* **1996**, *123*, 186.
(32) Vogt, T.; Buttrey, D. J. *Phys. Rev. B* **1995**, *52*, R9843.
(33) Huang, Q.; Soubeyroux, J. L.; Chmaissem, O.; Natali Sora, I.; Santoro, A.; Cava, R. J.; Krajewski, J. J.; Peck, W. F., Jr. *J. Solid State Chem.* **1994**, *112*, 355.
(34) Shaked, H.; Jorgensen, J. D.; Chmaissem, O.; Ikeda, S.; Maeno, Y. *J. Solid State Chem.* **2000**, *154*, 361.
(35) Shimura, T.; Itoh, M.; Inaguma, Y.; Nakamura, T. *Phys. Rev. B* **1994**, *49*, 5591.

Table 2. Atomic Coordinates and Isotropic Displacement Parameters for $Sr_4Rh_3O_{10}$ at Room Temperature (first lines) and 3.5 K (second lines)[a]

atom	site	*x*	*y*	*z*	$100U_{iso}$ (Å^2)	*n*
Sr1	4f	0.5	0	0.07083(26)	1.051(88)	1
				0.06963(26)	0.353(62)	
Sr2	4f	0.5	0	0.20379(20)	1.051(88)	1
				0.20410(19)	0.353(62)	
Sr3	4e	0	0	0.29621(20)	1.051(88)	1
				0.29590(19)	0.353(62)	
Sr4	4e	0	0	0.42917(26)	1.051(88)	1
				0.43037(26)	0.353(62)	
Rh1	2a	0	0	0	0.562(98)	1
					0.330(79)	
Rh2	4e	0	0	0.13880(24)	0.562(98)	1
				0.13991(25)	0.330(79)	
Rh3	4f	0.5	0	0.36120(24)	0.562(98)	1
				0.36009(25)	0.330(79)	
Rh4	2d	0.5	0	0.5	0.562(98)	1
					0.330(79)	
O1	4g	0.2986(14)	0.2014(14)	0	1.30(11)	1
		0.3050(13)	0.1950(13)		0.581(77)	
O2	8i	0.2049(8)	0.2951(8)	0.13800(25)	1.30(11)	1
		0.20263(68)	0.29737(68)	0.13791(23)	0.581(77)	
O3	8i	0.2951(8)	0.2951(8)	0.36200(25)	1.30(11)	0.191(27)
		0.29737(68)	0.29737(68)	0.36209(23)	0.581(77)	0.195(25)
O3′	8i	0.2049(8)	0.2049(8)	0.36200(25)	1.30(11)	0.809(27)
		0.20263(68)	0.20263(68)	0.36209(23)	0.581(77)	0.805(25)
O4	4h	0.2014(14)	0.2014(14)	0.5	1.30(11)	0.191(27)
		0.1950(13)	0.1950(13)		0.581(77)	0.195(25)
O4′	4h	0.2986(14)	0.2986(14)	0.5	1.30(11)	0.809(27)
		0.3050(13)	0.3050(13)		0.581(77)	0.805(25)
O5	4e	0	0	0.0701(4)	1.79(10)	1
				0.07001(32)	1.150(74)	
O6	4e	0	0	0.20913(27)	1.79(10)	1
				0.20947(27)	1.150(74)	
O7	4f	0.5	0	0.29087(27)	1.79(10)	1
				0.29053(27)	1.150(74)	
O8	4f	0.5	0	0.4299(4)	1.79(10)	1
				0.42999(32)	1.150(74)	

[a] The thermal parameters of the each set of oxygen (O1−4′ and O5−8) and the each metal were grouped and refined together. The atoms O3′ and O4′ were introduced by assuming the stacking faults with some constraints, as was done in the analogous ruthenium oxide $Sr_4Ru_3O_{10}$.[23] Other constraints set in this study were z(Sr1) + z(Sr4) = 0.5, z(Sr2) + z(Sr3) = 0.5, z(Rh2) + z(Rh3) = 0.5, z(O2) + z(O3) = 0.5, z(O5) + z(O8) = 0.5, z(O6) + z(O7) = 0.5, x(O1) + x(O4) = 0.5, x(O2) + x(O3) = 0.5, x(O1) + y(O1) = 0.5, x(O2) + y(O2) = 0.5, x(O3) = y(O3), and x(O4) = y(O4).

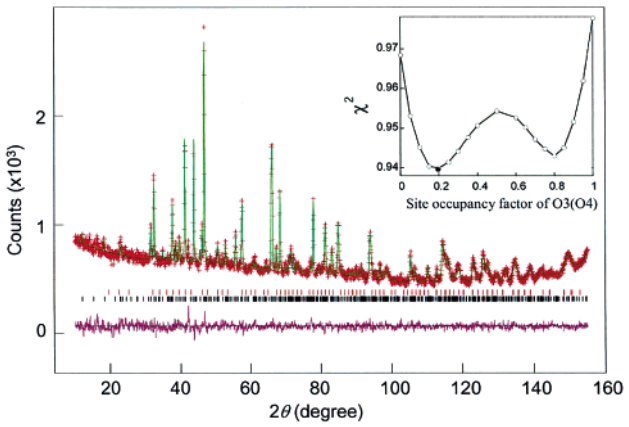

Figure 2. Neutron diffraction profile of the $Sr_4Rh_3O_{10}$ sample at 3.5 K. Vertical bars (black) indicate allowed Bragg reflections based on the orthorhombic (*Pbam*) structure model for $Sr_4Rh_3O_{10}$. The minor impurity (identified as $SrRhO_3$) was considered in the analysis as well: the vertical bars (red) indicate the allowed Bragg reflections. The difference between the calculation (green lines) and the raw data (red crosses) is shown below the bars. The inset shows variations of the reduced χ^2 for the fixed occupancy factors of O3 or O4 (open circle) and the unfixed solution (solid circle).

data previously published for Sr_2RhO_4 by others, a corresponding anomaly was not obvious.[12,35] Again, the small amount of the impurity phase may be responsible for this feature, and the details of this shall be left for future work.

Magnetic susceptibility data of $Sr_4Rh_3O_{10}$ are shown in Figure 6 along with the data for the other family members. The field dependence of the magnetization at 5 K is shown in the small panel. The sample holder correction was negligibly small and, therefore, not subtracted from the raw data. As expected, the curve for $Sr_4Rh_3O_{10}$ lies intermediate between those for the perovskite $SrRhO_3$ and the bilayered perovskite $Sr_3Rh_2O_7$. The weakly temperature dependent character therefore must represent mainly the magnetism of $Sr_4Rh_3O_{10}$, although the data do contain impurity contributions at a low level. The susceptibility of $Sr_4Rh_3O_{10}$ was approximately 1×10^{-3} emu/mol of Rh, which is much larger than that of normal metals. The susceptibility is then likely enhanced somewhat by substantial electron correlations, as found in $SrRhO_3$[14,20] and $Sr_3Rh_2O_7$.[15,36] To clarify this issue, a band structure calculation study on $Sr_4Rh_3O_{10}$ is in progress, which can provide information about noncorrelated magnetic susceptibility.

Specific heat data are plotted as C_p/T vs T^2 in Figure 7 with the data for other members. The data for $Sr_4Rh_3O_{10}$ were analyzed in a well-established manner, as

(36) Arai, M. Unpublished.

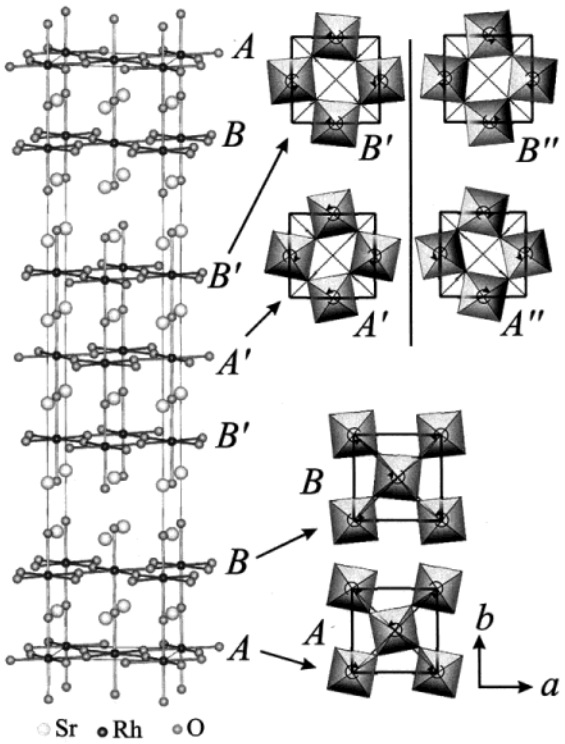

Figure 3. Structural view of $Sr_4Rh_3O_{10}$. Fine lines signify the orthorhombic unit cell. Cooperative rotations along the *c*-axis of the RhO_6 octahedra are indicated by circular arrows. Approximately a 20% stacking error, such as *A*″(*B*″) at *A*′(*B*′) blocks, was indicated by the neutron diffraction study. The tilting of each RhO_6 octahedron was ∼12° along the *c*-axis.

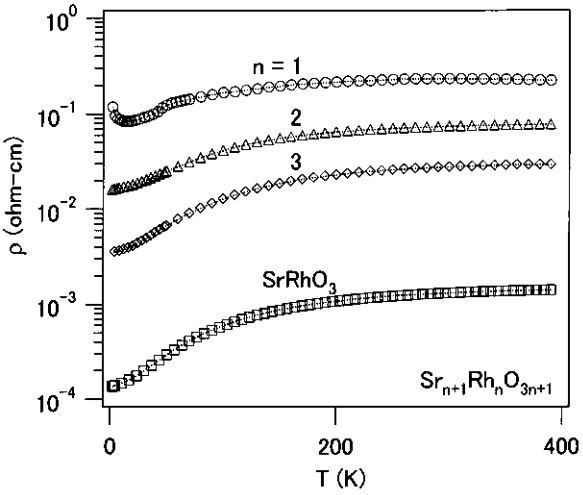

Figure 4. Temperature dependence of the resistivity of the Ruddlesden−Popper-type rhodates $Sr_{n+1}Rh_nO_{3n+1}$ ($n = 1$, 2, 3, and ∞). The data for the $n = 2$ and ∞ members were taken from our previous reports.[14,15]

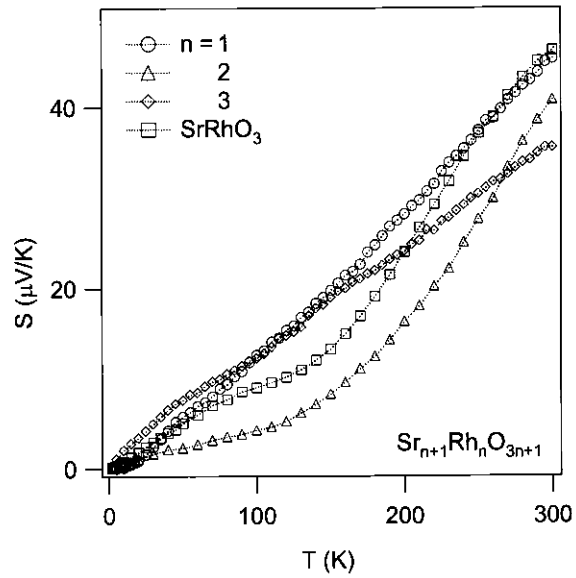

Figure 5. Thermoelectric property of the polycrystalline $Sr_4Rh_3O_{10}$ and Sr_2RhO_4. The data for the other members were taken from our previous reports.[14,15]

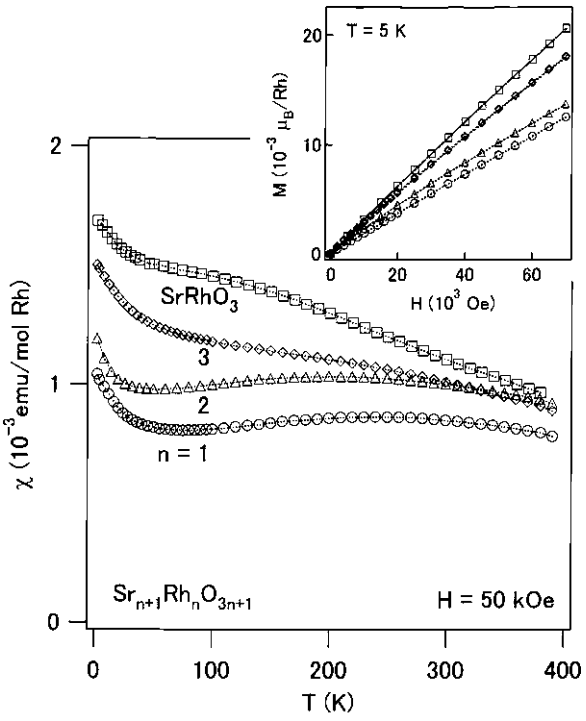

Figure 6. Temperature dependence of the magnetic susceptibility of the polycrystalline samples of $Sr_{n+1}Rh_nO_{3n+1}$ ($n = 1$, 2, 3, and ∞) at 50 kOe and applied magnetic field dependence of the magnetization at 5 K (small panel).

well as those for the other members.[14,15,37] The analytic formula applied in the low-temperature limit ($T \ll \Theta_D$) was

$$C_v/T = \gamma + 2.4\pi^4 r N_0 k_B (1/\Theta^3_D) T^2$$

where k_B, N_0, and r are the Boltzmann constant, Avogadro's constant, and the number of atoms per formula unit, respectively. The two parameters γ (electronic specific-heat coefficient) and Θ_D (Debye temperature) are material dependent in nature. The difference between C_p and C_v was assumed to be insignificant in the temperature range studied. As you can see in the above formula, probable magnetic contributions, which are expected by analogy with the previous results,[14,15,37] were not considered, because reliable magnetic terms were not clearly established.[2] This attempt is, therefore, a preliminary analysis.

The γ and Θ_D for $Sr_4Rh_3O_{10}$ were then estimated to be 16.13(7) mJ/mol of Rh K^2 and 355.3(5) K, respec-

(37) Yamaura, K.; Young, D. P.; Takayama-Muromachi, E. *Phys. Rev. B* **2004**, *69*, 024410.

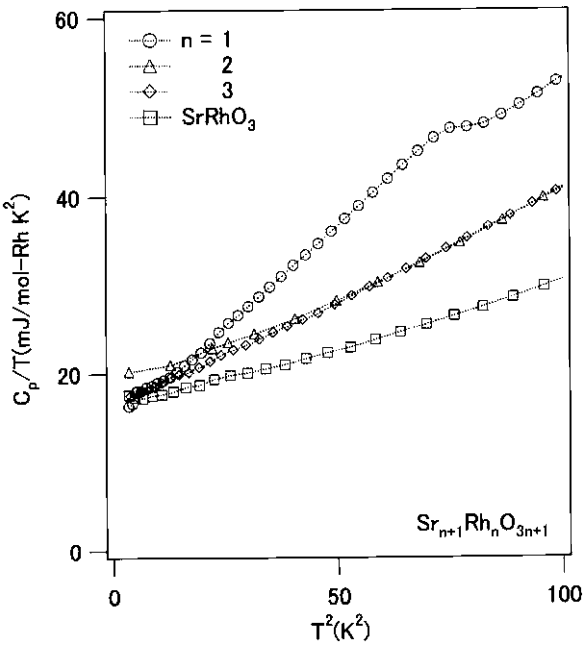

Figure 7. Specific heat of the polycrystalline samples of $Sr_{n+1}Rh_nO_{3n+1}$ (n = 1, 2, 3, and ∞). The data are plotted in C_p/T vs T^2 form. Dotted curves are guides to the eye. The data for the n = 2 and ∞ members were taken from our previous reports.[15,37]

tively, by a least-squares method with the linear part between 30 and 100 K^2 (5.4 K< T < 10 K). Unfortunately, estimation of the specific-heat parameters for Sr_2RhO_4 was problematic due to a small feature in the data that prevents us from analyzing the Sr_2RhO_4 data in the same manner. To determine what properties are associated with the anomaly, we looked for relevant information, as the compound was already studied by others. However, no prior specific-heat data were found in the literature. The Sr_2RhO_4 sample was then reinvestigated in a magnetic field of 70 kOe. In the magnetic study, the feature was found to be rather robust against the applied magnetic field. Although the data did not provide any definitive explanation for the feature, we naively assumed it possibly originated from the nature of Sr_2RhO_4. In the improved resistivity data (Figure 4), a small upturn was found at the low temperature, which might be associated with the feature. Future studies will make clear whether the assumption is correct. In the plots, the γ-value of all the members roughly congregate in a relatively narrow region of 12−18 mJ/mol of Rh K^2, directly indicating that all hold a certain level of electron correlation, because γ for free electrons is much lower.[20,36,38] This result roughly follows with what was suggested in the magnetic susceptibility study.

Here we go back to the structural chemistry. There are two major factors that characterize the local structure environments: amplitude of the cooperative rotations of RhO_6 octahedra and the frequency of the rotation-tilt errors. These factors might seriously affect the magnetism variations of the series. So far, structure studies revealed that the tilt angle of the RhO_6 octahedra was 10.3°, 10.5°, 11.0°, and 11.7° for n = 1, 2, 3, and ∞ for $Sr_{n+1}Rh_nO_{3n+1}$, respectively (this angle for $SrRhO_3$ is the larger of the two caused by the $GdFeO_3$-type distortion[14]). The tilting distortions are somewhat larger than those for the relevant ruthenates, 0°, 6.8°, 5.6°, and 8.6° for n = 1, 2, 3, and ∞[39] for $Sr_{n+1}Ru_nO_{3n+1}$, respectively. As was suggested in previous work, magnetically ordered states in these materials may depend sensitively on the degree of the tilt distortion; the most well-studied example can be found in $CaRuO_3$, where the tilt angle is large at ∼15.5° and the possible ferromagnetic order has totally disappeared.[40−44] We also found that approximately 20% of the perovskite blocks were out of regular RhO_6 tilting sequence. It is not clear how the rotation disorders affect the electron transport, as both disorders and impurities can reduce electron coherency.[45,46] The depressed local structure environments in the rhodates likely give a plausible explanation why this family of materials does not show rich magnetic behavior, while the ruthenate family does.

In summary, the trilayered rhodate $Sr_4Rh_3O_{10}$ was studied by neutron diffraction, followed by magnetic and electrical studies. Magnetic data for $Sr_4Rh_3O_{10}$ and the other members clearly showed that the rhodate family has a rather small variation in magnetic behavior in comparison with the ruthenate family. Considering the structure data for both families, it appears that the larger magnitude of local structure distortions and the frequent rotation-tilt disorders are likely responsible for the small variation in magnetism across the Rh series. In fact, non-*s* symmetry superconductivity was observed only in highly coherent crystals of the nondistorted, layered perovskite Sr_2RuO_4.[2] Further experimental efforts on the rhodate family will be necessary to explore for the possible appearance of quantum magnetic characters. For example, Ba-substitution might be effective in improving the local structure environment.

Acknowledgment. We wish to thank M. Akaishi (NIMS) for the high-pressure experiments, H. Aoki (NIMS) and H. Komori (NIMS) for EDS, and K. Kosuda (NIMS) for EPMA of the samples. This research was supported in part by the Superconducting Materials Research Project, administrated by the Ministry of Education, Culture, Sports, Science and Technology of Japan.

Supporting Information Available: Crystallographic information files (CIF) for $Sr_4Rh_3O_{10}$, at room temperature and 3.5 K, and tables for selected bond distances and angles in $Sr_4Rh_3O_{10}$ (PDF). This material is available free of charge via the Internet at http://pubs.acs.org.

CM0491072

(38) Hase, I.; Nishihara, Y. *J. Phys. Soc. Jpn.* **1996**, *65*, 3957.
(39) Jones, C. W.; Battle, P. D.; Lightfoot, P.; Harrison, W. T. A. *Acta Crystallogr.* **1989**, *C45*, 365.
(40) He, T.; Huang, Q.; Cava, R. J. *Phys. Rev. B* **2001**, *63*, 024402.
(41) Mazin, I.; Singh, D. J. *Phys. Rev. B* **1997**, *56*, 2556.
(42) Santi, G.; Jarlborg, T. *J. Phys.: Condens. Matter* **1997**, *9*, 9563.
(43) Fernanda, M. C.; Greatrex, R.; Greenwood, N. N. *Solid State Chem.* **1977**, *20*, 381.
(44) Longo, J. M.; Raccah, P. M.; Goodenough, J. B. *J. Appl. Phys.* **1968**, *39*, 1327.
(45) Larkin, A. I. *JETP Lett.* **1965**, *2*, 130.
(46) Balian, R.; Werthamer, N. R. *Phys Rev.* **1963**, *131*, 1553.